European Coordination for Accelerator Research and Development

PUBLICATION

Magnetic Design and Code Benchmarking of the SMC (Short Model Coil) Dipole Magnet

Manil, P (CEA) *et al*

18 December 2009

The research leading to these results has received funding from the European Commission under the FP7 Research Infrastructures project EuCARD, grant agreement no. 227579.

This work is part of EuCARD Work Package **7: Super-conducting High Field Magnets for higher luminosities and energies**.

The electronic version of this EuCARD Publication is available via the EuCARD web site <http://cern.ch/eucard> or on the CERN Document Server at the following URL : <http://cdsweb.cern.ch/record/1229432>

Magnetic Design and Code Benchmarking of the SMC (Short Model Coil) Dipole Magnet

Pierre Manil, Federico Regis, James Rochford, Paolo Fessia, Simon Canfer,
Elwyn Baynham, François Nunio, Gijs de Rijk, Pierre Védrine

***Abstract*— The Short Model Coil (SMC) working group was set in February 2007 within the Next European Dipole (NED) program, in order to develop a short-scale model of a Nb_3Sn dipole magnet. The SMC group comprises four laboratories: CERN/TE-MSC group (CH), CEA/IRFU (FR), RAL (UK) and LBNL (US). The SMC magnet is designed to reach a peak field of about 13 Tesla (T) on conductor, using a 2500 A/mm^2 Powder-In-Tube (PIT) strand. The aim of this magnet device is to study the degradation of the magnetic properties of the Nb_3Sn cable, by applying different levels of pre-stress. To fully satisfy this purpose, a versatile and easy-to-assemble structure has been realized. The design of the SMC magnet has been developed from an existing dipole magnet, the SD01, designed, built and tested at LBNL with support from CEA. The goal of the magnetic design presented in this paper is to match the high field region with the high stress region, located along the dipole straight section. For this purpose, three-dimensional nonlinear parametric models have been implemented using three codes (CAST3M, ANSYS™, and OPERA™). This optimization process has been an opportunity to cross-check the codes. The results of this benchmarking are presented here, along with the final design which incorporates the use of end spacers and a surrounding iron structure to deliver a nominal field of 13 T uniformly distributed along the cable straight section.**

***Index Terms*— Dipoles, magnetic design, models cross-check, Nb_3Sn, superconducting accelerator magnets.**

I. Introduction

FUTURE dipole magnet upgrades, requiring higher fields in larger apertures, will demand the use of a superconductor with greater performance compared to Nb-Ti, such as Nb_3Sn. This material is brittle and strain-sensitive. Its upper stress limit is estimated to be approximately 150 MPa, but the behavior of Nb_3Sn insulated cables in coils is not fully understood. Improving this knowledge is essential for magnet designers because the higher magnetic fields generate large Lorentz forces and large stresses on the coil. The goal of the SMC working group is to create a subscale Nb_3Sn dipole test bed where different levels of pre-stress can be applied to the coil. Varying the pre-stress makes it possible to explore both the mechanical limit of the Nb_3Sn before degradation and the impact of a low pre-stress on the magnet training performance.

Several Nb_3Sn magnets have been tested in the US since 1997 [1]-[4] within the High Field Magnets and LARP programs. In Europe, in January 2008, the HFM (High Field Magnets) took over the NED program, which was mainly focused on the Nb_3Sn cable development [5]-[7]. Within the framework of the European project EuCARD, the SMC is the first European test dipole using the Nb_3Sn conductor. It takes over the same design principles as the SD01 [8], a racetrack dipole coil tested at LBNL.

As for SD01, the SMC subscale dipole is racetrack-shaped. It is made of two Nb_3Sn Rutherford cable layers wound around a metallic pole (double pancake configuration). A thin insulation sheet is placed between both pancakes. The whole dipole magnet consists in two double pancakes separated by a mid-plane insulation layer made of glass-fiber epoxy composite. The racetrack configuration makes the winding process and the pre-stress application simpler. Before magnetization, the coil pack is inserted inside a mechanical support structure composed of a yoke, four pads and a cylindrical outer shell. The description of the SMC structure and the reasons behind this mechanical design have been reported in [9].

II. Model Constraints and Parameterization

The superconducting cable features have been fixed at an early stage on the base of the NED specifications. The SMC Rutherford-type cable has 14 PIT strands with a diameter of 1.25 mm. It has a rectangular section of 9.7 x 2.2 mm, plus 0.2 mm per face for the epoxy insulation in the baseline configuration, as shown in Fig. 1.

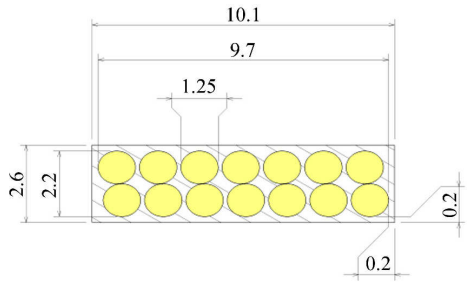

Fig. 1. Schematic view of the SMC cable cross-section (values in mm).

Manuscript received 18 October 2009.

P. Manil and F. Nunio are with CEA Saclay/IRFU/SIS; P. Védrine is with CEA Saclay/IRFU/SACM, 91191 Gif-sur-Yvette, France (phone: +33-1 69 08 74 79; e-mail: pierre.manil@cea.fr).

F. Regis, P. Fessia, G. de Rijk are with CERN (European Organization for Nuclear Research), Switzerland (e-mail: federico.regis@cern.ch).

J. Rochford, S. Canfer and E. Baynham are with RAL/STFC, Harwell Science and Innovation Campus, Didcot, United Kingdom (e-mail: james.rochford@stfc.ac.uk).

The target practical strand current density at 12 T and 4.2 K is 2500 A/mm^2, corresponding to an engineering current density J_{eng} around 654 A/mm^2. The critical current slope α_c has been linearized around 12 T [7]. Those properties are summarized in Table I. At a later stage, different insulation types such as an innovative ceramic insulation [10] could be used, implying slight changes in the magnetic design.

TABLE I. SMC CABLE PROPERTIES

Parameter	Symbol	Unit	Value
Number of strands	N_{str}	/	14
Strand diameter	$Ø_{str}$	mm	1.25
Cu / nCu rate	$r_{Cu/nCu}$	/	1.25
Twist pitch	p	mm	60
Bare cable width	w_{cbl}	mm	9.7
Bare cable thickness at a stress of 20 MPa	t_{cbl}	mm	2.20
Epoxy insulation thickness per face	t_{ins}	mm	0.2
Critical current slope at 12 T	α_c	A/T	-3435
Critical current density slope at 12 T	α_J	A/mm²/T	-450
Target current density at 12 T, 4.2 K	J_{trg}	A/mm²	2500

It is proposed to match the peak magnetic field region with the high stress zone, in the middle of the straight section, where the cable performance is not reduced by the winding deformation. Doing this, we make sure that the conductor is as much mechanically homogeneous as possible, and we try to control the mechanical effects that will affect the magnet training and performances. In the following study, the field magnitude $|B|$ is always considered.

The peak field B_{max}, in the center of the straight section of the racetrack, should approach 13 T at short sample limit. The magnetic peak field on the ends B_{end} should be at least 0.5 T lower than the one on the straight section center B_{ss}. The uniformity of the field in this zone should be better than 1% over a full twist pitch length p. There is no constraint on the central field B_0, neither on the field harmonics. In addition to these magnetic specifications, the working current is limited to 20 kA by the available power supply. The coil dimensions should remain limited. Additionally, there are implicit cost constraints. Those specifications are summarized in Table II.

TABLE II. SMC MAGNETIC SPECIFICATIONS

Parameter	Symbol	Unit	Specified value
Peak field localization	/	/	straight section
Peak field	B_{max}	T	13
Straight-end field difference	ΔB	T	≥ 0.5
Central field	B_0	T	none
Uniform field zone length at 1%	$L_u^{1\%}$	mm	~ 60
Short-sample limit current	I_{ss}	kA	≤ 20
Overall length	L_{tot}	mm	limited
Overall width	w_{tot}	mm	limited

The following magnetic optimization is focused on: the overall number of turns N_{tot}, the number of end spacers N_s on each side, the spacers' axial lengths L_i (i = [1;N_s]), the number of turns in each block N_j (j = [1;N_s+1]), the pole half-width r_{int}, the straight section length L, the interlayer insulation thickness t_{int} and the mid-plane insulation thickness t_{mid}. Those parameters are represented in Fig. 2 for a particular case.

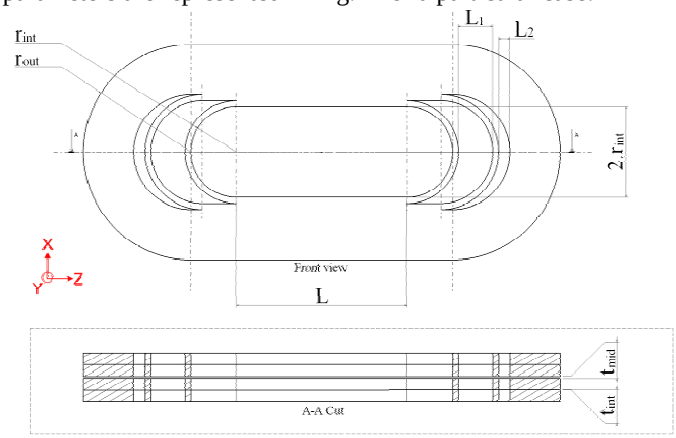

Fig. 2. SMC coil pack parameters.

III. MODELING METHOD

The magnetic optimization has been performed in parallel with the Finite Element Method codes CAST3M (CEA) [11], ANSYS (CERN), and OPERA (RAL) with frequent cross-checks. The duplicated calculations primarily served to validate the computations, and secondly they allowed the different institutes to benchmark the validity of their individual modeling processes.

The procedures used in CAST3M and OPERA are quite similar. The source field calculations are based on the semi-analytic Biot-Savart formulation, applied to the coil geometry divided into canonical sub-elements (bars and arcs) independent from the mesh. With iron, the Magnetic Scalar Potential (MSP) approach is considered, using the total scalar potential in regions which contain permeable materials (iron and air) and the reduced scalar potential in regions which contain source currents (coil and air). Both regions are fully meshed. The nonlinear iron characteristics are entered as a table of point values. On the interface surface between these regions, the two scalar potentials are linked together by applying the conditions of normal flux density and tangential magnetic field intensity continuity. The contributions of the current sources and the iron regions are added together in the post processing module to generate the final field distribution.

In ANSYS, two different approaches are followed: the Magnetic Vector Potential (MVP) and the MSP. The first approach is used for general assessment computations, whereas the second for the optimized configuration only. A model using the MVP formulation is faster to build and allows a direct computation of the Lorentz forces on the mesh. Nevertheless it could give incorrect results when nonlinear magnetic effects are included (iron saturation). The MSP approach allows performing faster simulations (one degree of freedom per element node instead of three), but it requires an electro-magnetic analysis in order to compute the coil current density to finally get the Lorentz forces.

IV. Parametric Study

A. Number of Turns

The influence of N_{tot} on B_{max} is studied on a baseline set of parameters inspired from SD01. Without end spacer, $N_{tot} \geq 17$ is necessary for B_{max} to reach 13 T. In this case, the peak field is located in the ends. With one spacer, N_{tot} must be larger than 19, as showed on Fig. 3. For instance, with N_{tot} = 20, the use of one end spacer reduces B_{max} by about 0.25 T.

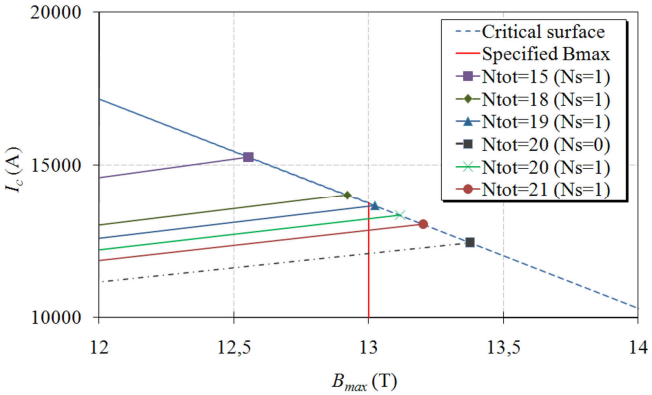

Fig. 3. Influence of N_{tot} on the magnet load lines with no spacer (N_s=0) or with one spacer (N_s=1, L_1=10 mm, N_1=2). No iron is considered here. The other parameters are set as listed in [12].

B. Coil Pack Parameters

It is showed that r_{int} should be as small as possible in terms of magnetic efficiency. For a fixed N_{tot}, a smaller r_{int} leads to higher B_{max} with lower ΔB [12]. On the other hand, r_{int} needs to be large enough to avoid bending issues, such as cable pop-outs that could damage the cable. From the experience of SD01, we consider that 32.8 mm is the minimal value (by scaling r_{int} with respect to the cable thickness ratio). We decide to allow a safety margin by setting r_{int} to 40 mm.

Fig. 4 shows that increasing L reduces the effect of the ends on the straight section and improves the field uniformity. On the other hand, L must remain short enough to make sure that the coil pack fits inside the furnace available. L is fixed to 150 mm so that $L_u^{1\%} \sim p$.

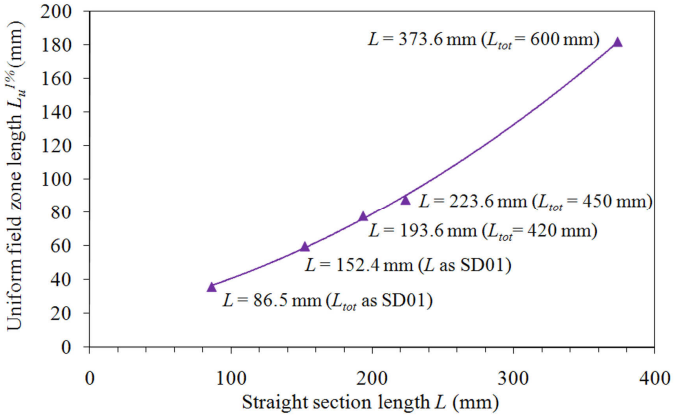

Fig. 4. Influence of L on the uniform field zone length $L_u^{1\%}$.

The insulation thicknesses are shown to have a second order influence on the resulting field. For practical reasons, t_{mid} is fixed to 1.6 mm and t_{int} to 0.2 mm. At this stage, the peak field remains located in the ends.

C. End Spacers

It is proposed to add spacers in the magnet ends. Doing this, we expect to decrease significantly B_{end} while keeping B_{ss} almost unchanged. Configurations with zero, one, or two end spacers per side are considered. For a fixed current of 14 kA, Table III shows that the most efficient configuration in terms of ΔB is for N_s=2. N_{tot} is fixed to 21. The best configuration is obtained for N_1=N_2=2 (i.e. N_3=17), with L_1=30 mm and L_2= 10 mm [12]. The peak field is still located in the ends.

TABLE III. End Spacers Influence on Magnetic Results

Parameter	Unit	N_s=0	N_s=1	N_s=2
L_1	mm	/	40	30
L_2	mm	/	/	10
B_{ss}	T	11.41	11.10	11.11
B_{end}	T	13.78	12.51	11.66
ΔB	T	-2.37	-1.41	-0.55

D. Iron Parts

Using iron parts along the straight section of the magnet will help concentrate the flux lines in this region. It is proposed to take advantage of the SMC structure by making some of its parts in MAGNETIL® iron. Different cases are investigated: no iron (set 0); iron yoke (set 1); iron yoke and vertical pads (set 2); iron yoke and all pads (set 3). Contrary to SD01, a non-magnetic pole is preferred. In every case, the iron covers 70% of L, i.e. 105 mm. Table IV shows at I_{ss} that the simplest suitable solution is obtained with the set 2.

TABLE IV. Iron Parts Influence on Magnetic Results

Parameter	Unit	Set 0	Set 1	Set 2	Set 3
B_{ss}	T	12.00	12.16	12.91	12.94
B_{end}	T	12.60	12.69	12.26	12.27
ΔB	T	-0.60	-0.53	0.64	0.67

The previous parametric study leads to the final set of parameters presented in Table V.

TABLE V. SMC Optimized Parameters

Parameter	Symbol	Unit	Value
Number of turns	N_{tot}	/	21
Number of end spacers	N_s	/	2
Axial length of the inner spacer	L_1	mm	30
Axial length of the outer spacer	L_2	mm	10
Number of turns in the inner block	N_1	/	2
Number of turns in the mid-block	N_2	/	2
Pole half-width	r_{int}	mm	40
Straight section length	L	mm	150
Interlayer insulation thickness	t_{int}	mm	0.2
Mid-plane insulation thickness	t_{mid}	mm	1.6

V. Final Results and Code Benchmarking

The magnet design process was an iterative one, with the different laboratories using four different magnetic design formulations. The previous analysis has voluntarily been presented straight-forward, without pointing the codes used. The final magnetic results, based on the optimized set of parameters, are compared in Table VI.

TABLE VI. SMC Magnetic Results Comparison

Parameter	Unit	Target	CAST3M MSP	OPERA MSP	ANSYS MSP	ANSYS MVP
B_{max}	T	13	12.92	12.96	12.94	12.85
B_{end}	T	≤ 12.5	12.22	12.23	12.22	12.20
ΔB	T	≥ 0.5	0.70	0.73	0.71	0.71
B_0	T	none	9.93	9.80	9.65	9.85
$L_u^{1\%}$	mm	~ 60	~ 70	~ 60	~ 55	~ 55
I_{ss}	kA	≤ 20	14.01	14.00	13.96	14.25
Forces (F_X)	MN/m		1.9	2.0	2.0	2.1
Forces (F_Y)	MN/m		-1.8	-1.9	-1.9	-1.9
Stored energy	kJ		211	209	190	198
Inductance	mH		2.1	2.1	1.9	2.0

A first glance shows a good agreement between all four models. Discrepancies below 1% are observed on B_{max} and B_{end}, and below 3% on B_0. They can be explained partly by the mesh effect influencing the local peak values, and partly by the formulation choice [12]. The discrepancy is lower between the three MSP models, around 0.3%. This can be explained by the source conductor definition which follows the same semi-analytical approach in those cases [13]. Despite the differences in magnetic formulations, model features, and numerical solvers, the results appear to be in very good agreement everywhere on the coil. The four models lead to the same optimized solution. The field magnitude distribution inside the coil is represented in Fig. 5 along three particular turns. This plot highlights the influence of the iron parts on the peak field location.

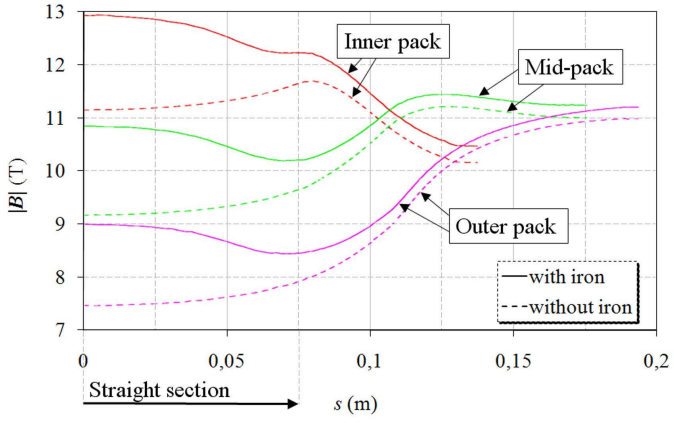

Fig. 5. Magnetic field magnitude distribution inside the coil along turn 1 (inner pack), turn 3 (mid-pack) and turn 5 (outer pack) at I_{ss} with and without iron parts (CAST3M). *s* is the curvilinear abscissa along the cable; s = 0 in the center of the straight section of the magnet.

VI. Conclusion

The magnetic optimization of the SMC racetrack magnet has been presented on the base of the NED cable. Using the SD01 subscale dipole as a starting point, the SMC study has shown: optimizing the number of turns and the coil pack features; using two end spacers on each side; using a non-magnetic pole; optimizing the iron parts. The resulting magnetic field has a maximum around 13 T located as desired on the dipole straight section, for a quench current around 14 kA. This peak field shows a significant margin compared to the ends (over 0.7 T) and a good uniformity over a twist pitch. The final coil pack is approximately 420 mm-long, 190 mm-wide and 42 mm-thick. This configuration is ideal for the future training studies with variable mechanical pre-stresses.

The magnetic field computations have been cross-checked between CAST3M, OPERA, and ANSYS (MSP and MVP formulations). Those four nonlinear models lead to the same conclusions in terms of magnet design.

The next step has been to calculate and to design an adapted mechanical test bed. This structure has been built and instrumented. It is being calibrated, before the first full magnet tests programmed for the beginning of 2010.

Acknowledgment

The authors would like to thank Arnaud Devred (ITER), Hélène Félice, Paolo Ferracin, Shlomo Caspi, Ray Hafalia (LBNL) and François-Paul Juster (CEA/IRFU).

References

[1] A. Lietzke, *et al.*, "Test results of RD3c, a Nb_3Sn common-coil racetrack dipole magnet," *IEEE Trans. Applied Superconductivity*, vol. 13, Part 2, pp. 1292–1296, 2003.

[2] S. Mattafirri, *et al.*, "Performance analysis of HD1: a 16 T Nb_3Sn dipole magnet," *IEEE Trans. Applied Superconductivity*, vol. 15, Part 2, pp. 1156–1159, 2005.

[3] S. Caspi, *et al.*, "Test Results of LARP Nb_3Sn Quadrupole Magnets Using a Shell-Based Support Structure (TQS)," *IEEE Trans. Applied Superconductivity*, vol. 19, issue 3, Part 2, pp. 1221–1225, June 2009.

[4] A. Zlobin, *et al.*, "R&D of Nb_3Sn accelerator magnets at Fermilab," *IEEE Trans. Applied Superconductivity*, vol. 15, Part 2, pp. 1113–1118, 2005.

[5] A. Devred, *et al.*, "Overview and status of the Next European Dipole (NED) joint research activity," *Supercond. Sci. Technol.*, vol. 19, 2006.

[6] T. Boutboul, *et al.*, "Nb3Sn conductor development and characterization for NED," *J. Phys.: Conf. Ser.*, vol. 97, 2008.

[7] A. Devred, *et al.*, "Status of NED conductor development," presented at *IEEE/CSC & ESAS Europ. Superconductivity News Forum*, 2007, ST5.

[8] H. Félice, *et al.*, "Design and test of a Nb_3Sn subscale dipole magnet for training studies," *IEEE Trans. Applied Superconductivity*, vol. 17, Part 2, pp. 1144–1148, 2007.

[9] F. Regis, *et al.*, "Mechanical design of the SMC (Short Model Coil) dipole magnet," *IEEE Trans. Applied Superconductivity*, to be published.

[10] F. Rondeaux, "Insulation development: final report on innovative insulation," *CARE Report*, 2007-037-NED, 2007.

[11] P. Verpeaux, T. Charras, A. Millard, "Castem2000: une approche moderne du calcul des structures," *Calcul des Structures et Intelligence Artificielle*, p. 261. Pluralis, 1988.

[12] P. Manil, F. Regis, J. Rochford, *et al.*, "NED Short Model Coil project: technical note on magnetic design," *CEA/CERN Technical Report*, EDMS id: 926137, 2008.

[13] M. Gyimesi, D. Lavers, T. Pawlak, and D. Ostergaard, "Biot-Savart integration for bars and arcs," *IEEE Trans. Magnetics*, vol. 29, no. 6, pp. 2389-2391, 1993.